PHYSICAL REVIEW B VOLUME 22, NUMBER 6 15 SEPTEMBER 1980

Emission spectroscopy of alkali halide phosphors doped with s^2 ions: KI:Sn^{2+}

Y. Kamishina* and P. W. M. Jacobs
Department of Chemistry, University of Western Ontario, London, Canada N6A 5B7

D. J. Simkin, J.-P. Martin, and K. Oyama-Gannon
Department of Chemistry, McGill University, Montreal, Quebec, Canada H3A 2K6

D. Le Si Dang
Laboratoire de Spectrométrie Physique, Université Scientifique et Médicale de Grenoble, Boîte Postale 53, 38041 Grenoble, France
(Received 21 March 1980)

The dependence of the emission of KI:Sn^{2+} on crystal temperature and excitation wavelength is described, including the emergence of a new band (R) which peaks at 1.89 eV. The temperature dependence of the decay times and the effect of a magnetic field on the decay times is described for all three emission bands of KI:Sn^{2+} (A_{T1}, A_{T2}, and R). The results are interpreted in terms of a model that requires the electron-lattice interaction (Jahn-Teller effect) to be much stronger than the spin-orbit coupling, while a nearby cation vacancy supplies an additional, weak electrostatic perturbation. Evidence is presented that indicates that the new R emission band arises from Sn^{2+} dimers oriented along the ⟨110⟩ direction.

I. INTRODUCTION

Over the years a great deal of effort has been devoted to the study of the light emission from alkali halides (NaCl, KCl, etc.) activated by impurities of Tl^+-like ions with the electronic configuration ns^2 (Ga^+, In^+, Tl^+, Sn^{2+}, Pb^{2+}, etc.).[1] The details of this emission depend upon the interplay and relative magnitude of the various perturbations to which the Tl^+-like ion is subjected in the crystal. These include spin-orbit interaction, electron-lattice coupling (Jahn-Teller effect), and in the case of divalent activators (like Sn^{2+}) the effects of nearby charge-compensating cation vacancies. There have been numerous studies of Sn^{2+} centers in alkali halides,[2-14] and, from studies of polarized luminescence and Mössbauer effect, Zazubovich and his co-workers[7-10] were able to identify three types of Sn^{2+} centers in KCl and in KBr: isolated Sn^{2+} substitutional ions on a cation site (K^+) and, possibly, two kinds of Sn^{2+}-cation vacancy complexes. The two possible Sn^{2+}-cation vacancy complexes arise from the possibility of the cation vacancy occupying either the nearest-neighbor (NN) cation position (v_{NN} along a ⟨110⟩ direction) or the next-nearest-neighbor position (v_{NNN} along a ⟨100⟩ direction).

For the isolated Sn^{2+} centers, excitation into the A or B absorption bands results in a single emission band, A_T, while for the Sn^{2+}-vacancy complexes such excitation leads to two overlapping emission bands separated by about 0.2 eV. The two emission bands of the Sn^{2+}-vacancy complex will be referred to hereafter as A_{T1} and A_{T2}, in order of increasing energy. Two important insights into the nature of the relaxed excited states from which the emission arises have been gained from polarization studies[4,7-9]: (1) the vacancy effect is small compared to the spin-orbit (SO) and Jahn-Teller (JT) interactions and (2) the electron-lattice (or JT) coupling is to the E_g vibrational modes of the lattice. However, profound disagreement persists regarding the relative importance (magnitude) of the SO and JT interactions. Fukuda[4] has adopted a model based on SO > JT while Hizhnyakov and Zazubovich[9] have proposed the reverse: JT > SO. A better understanding of the relaxed excited state (RES) of Sn^{2+} centers requires further study of the emission. In this paper we present the results of studies of the dependence of the emission from KI:Sn^{2+} on temperature and excitation energy and of the decay kinetics of that emission as a function of both temperature and external magnetic field. Our results strongly support a model based on JT > SO for the RES of Sn^{2+} centers in KI.

II. EXPERIMENTAL

A. Emission spectra

Crystals of KI:Sn^{2+} grown by the Stockbarger method at the University of Western Ontario (UWO) had an absorption spectrum in the C- and D-band regions that differed significantly from that of two crystals kindly supplied by Professor A. Fukuda and Dr. P. H. Yuster, respectively. The presence of cation impurities in the UWO crystals was suspected, but neutron activation analysis revealed Br^- to be the only significant impurity. All three crystals showed similar emission spectra following A-band excitation. However, all the data to be

described in Secs. III and IV were obtained using cleaves cut from the crystal given to us by Professor Fukuda, so that valid comparisons could be made with the data in Refs. 4, 5, and 6. The cleaves, about 3 mm in thickness (quenched from 650 °C to room temperature) were mounted in an Oxford Instruments cryostat and irradiated with light from an Oriel 1000-W Xe-Hg arc lamp which had been passed through a $NiSo_4 + CoSO_4$ solution and a Jarrell-Ash 0.25-m monochromator. The radiation emitted at right angles to the incident beam was focused on the entrance slit of a 0.5-m Heath monochromator equipped with a GCA/McPherson programmable filter assembly and detected by a GaAs photomultiplier. The emission was measured with a photon-counting system employing a PAR/SSR 1110 digital synchronous computer. The wavelength of the Heath monochromator was varied by an automatic stepwise scanner, and the primary data, consisting of the number of counts at each wavelength, were passed to a DEC PDP-10 time-shared computer. The system was calibrated using a quartz-iodine standard lamp with an MgO reflector in place of the crystal, and all emission spectra were corrected for the dependence of the sensitivity of the system on wavelength. The emission spectra are plotted as emission line shape versus photon energy ($h\nu$), where emission line shape is the relative intensity of the emission divided by $(h\nu)^3$.

B. Decay-time measurements

The samples of KI:Sn^{2+} (quenched as for emission measurements) were mounted in an Oxford Instruments horizontal-bore superconducting magnet which produced fields of up to 5 T. The temperature of the crystal could be varied down to ~3 K. Luminescence was excited using the radiation from a Carver Corporation Model N300 pulsed nitrogen-laser ($\lambda = 337.1$ nm, pulse energy 50 μJ, pulse duration < 15 nsec) filtered through three Corning 7-54 uv band-pass filters. The luminescence was passed through an interference filter centered on a wavelength of 650, 550, or 500 nm and with a 10-nm bandwidth and then through a Corning 0-52 uv cutoff filter and finally focused on an EMI 9558QB photomultiplier. The photomultiplier output was amplified by a preamplifier with a rise time of less than 10 nsec and then recorded using a Biomation 805 transient recorder with a minimum channel width of 200 nsec.

III. EMISSION SPECTRA

The line shape of the emission from KI:Sn^{2+} excited at 330 nm (3.757 eV) at 13.5 K is shown in Fig. 1(a). The emission consists of the previously reported[1] A-band doublet A_{T1} and A_{T2} and a smaller band, which we call R (for red), peaking at 1.86 eV. The spectrum resolves well into three overlapping Gaussian bands. With increasing temperature [Figs. 1(b), 1(c), and 1(d)] the bands broaden and the intensity of the R band decreases relative to the A_{T1}, A_{T2} bands. The relative intensity of the A_{T1} and A_{T2} components probably does not change much with T up to 90 K, above which temperature the R band is indistinguishable and the A_{T1} and A_{T2} components cannot be resolved satisfactorily. The temperature dependence of the zeroth, first, and second moments is shown in Fig. 2 over the ranges for which the resolution could be considered satisfactory. The anomaly at ~55 K in the zeroth and first moments is probably due rather to errors in the deconvolution process than to any unusual physical phenomenon. The first moments are sensibly independent of T and yield band positions, extrapolated to 0 K, of $M_1(R) = 1.890$ eV, $M_1(A_{T1}) = 2.214$ eV, $M_1(A_{T2}) = 2.395$ eV, respectively.

The emission spectrum in the A_{T1}-, A_{T2}-band region at 14 K depends critically on excited wavelength λ_e as shown in Figs. 3 and 1(a). For $\lambda_e = 310$ nm, which lies just in the long-wavelength tail of the C band (see Fig. 4) where it overlaps the B band, the A_{T1} band is the most prominent emission, the R band is completely absent. At $\lambda_e = 320$ nm (still in the B absorption band) the R band begins to appear and the A_{T1}, A_{T2} peaks are of almost equal intensity. At $\lambda_e = 325$ nm, the A_{T2} peak is the more prominent and the R band well established [Fig. 3(b)]. At $\lambda_e = 330$ nm, which corresponds to the low-energy side of the B absorption band, the R band is most intense (as confirmed by its excitation spectrum[11]) and A_{T1} exceeds A_{T2} in intensity [Fig. 1(a)]. As λ_e is further increased, the R emission decreases and A_{T2} increases at the expense of A_{T1}, up to $\lambda_e = 350$ nm (the minimum in the A absorption band) after which A_{T1} increases again at the expense of A_{T2}. Figures 3(c) and 3(d) show the spectra for $\lambda_e = 345$ and 355 nm, respectively. It should be noted that the normalized spectra for $\lambda_e = 355$, 365, and 370 nm are superimposable and all show a very weak component at 2.73 eV. The origin of this emission band is not yet understood and will not be discussed in this paper.

From these rather complex results we may conclude the following.

(i) Both A_{T1} and A_{T2} emission bands can be excited within the A, B, or C absorption band. In particular, absorption into the low-energy side of the A band favors the low-energy emission A_{T1}, while for absorption into the high-energy side of the A band the reverse is true.

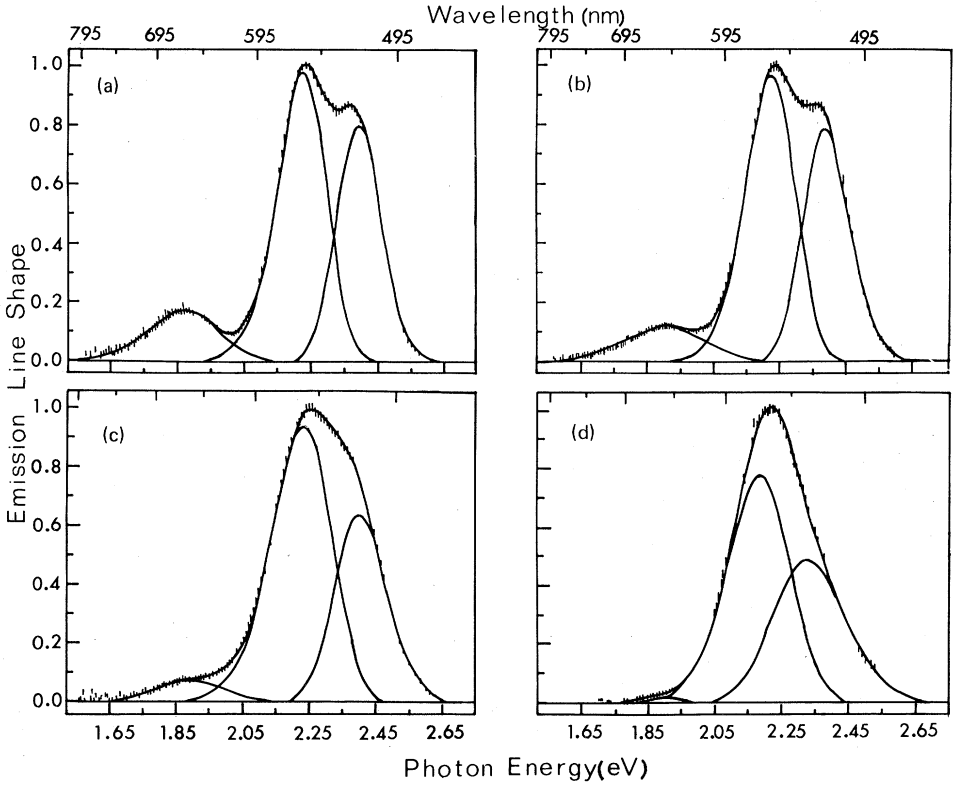

FIG. 1. Emission line shape as a function of photon energy for KI:Sn^{2+} excited at 330 nm. (a) $T=13.5$, (b) 29.6, (c) 59.7, and (d) 89 K.

(ii) The excitation of the R band is quite selective and occurs most efficiently in the low-energy side of the B band at 330 nm. It may also be excited in the D-band region, but does not appear at all when absorption occurs in the C band.

IV. DECAY TIMES

Pulsed excitation into the A absorption band of s^2 ions in alkali halides may be expected to result in a compound, two-component decay. However, in the case of KI:Sn^{2+}, only a single-decay time is observed for the A_{T1}, A_{T2}, and R emissions. A second, fast component may be present but may be either too weak or too short ($\lesssim 1$ μsec) to be observed with our experimental arrangement. The following discussion is based on the assumption that the observed decay time corresponds to the

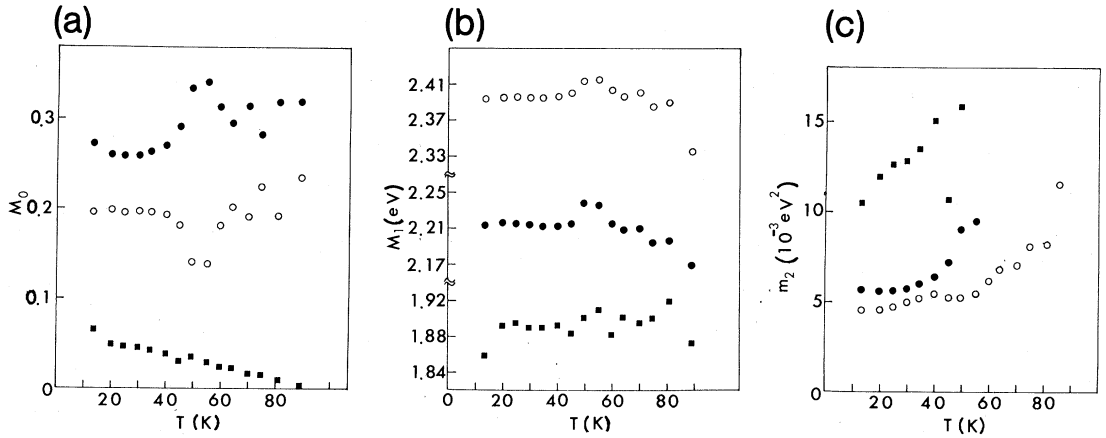

FIG. 2. The temperature dependence of zeroth, first, and second moments of the resolved (Gaussian) R■, A_{T1}●, and A_{T2}○ bands.

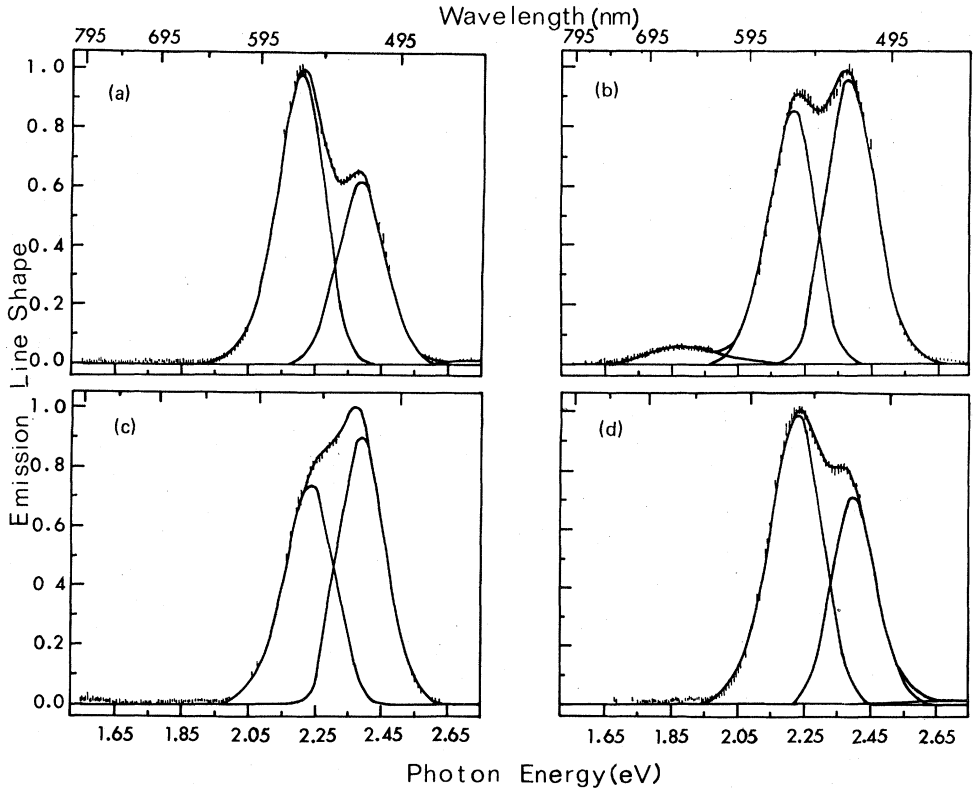

FIG. 3. The dependence of the emission from KI:Sn^{2+} on excitation wavelength (a) $\lambda_e = 310$, (b) 325, (c) 345, (d) 355 nm.

slow component and that the fast component, if present, is not detected.

The temperature dependence of the (slow) decay-time constant, τ, for A_{T1}, A_{T2}, and R is shown in Fig. 5. The decay times for both A_{T1} and A_{T2} were equal within our experimental error (~5%). The decay times of all three emission bands (A_{T1}, A_{T2}, and R) were temperature dependent with $\ln\tau \propto T^{-1}$ at high temperatures, but leveled off to a constant, limiting value at sufficiently low temperatures (see Fig. 5).

The effect of an applied magnetic field on the

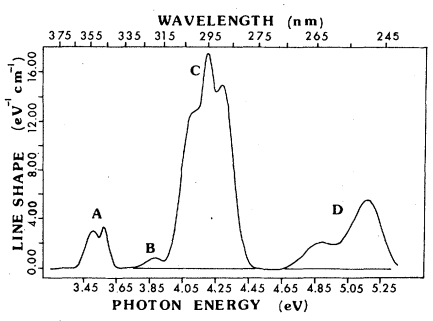

FIG. 4. Absorption spectrum of KI:Sn^{2+} at 15 K (from Ref. 11).

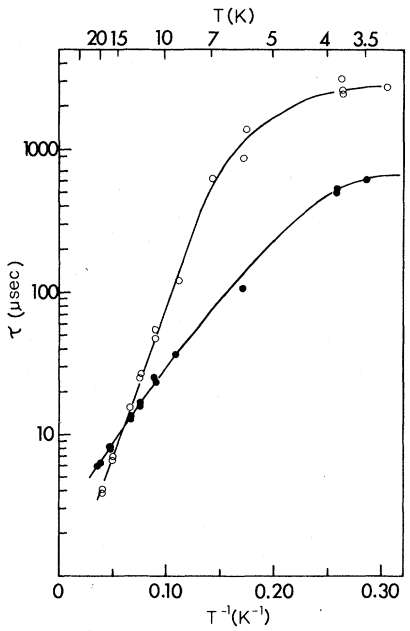

FIG. 5. The temperature dependence of the emission decay times of the A_{T1} and A_{T2} bands (open circles) and the R band (solid circles).

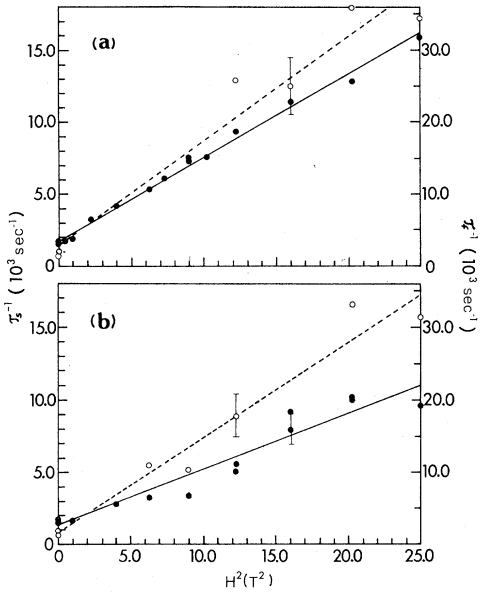

FIG. 6. The magnetic field dependence of the emission decay time of the R band (at ~3.3 K), (a) $\vec{H} \parallel \langle 100 \rangle$, (b) $\vec{H} \parallel \langle 111 \rangle$. Open circles, fast component (right-hand scale); filled circles, slow component (left-hand scale).

decay times was measured at $T = 3.3$ K. The application of a magnetic field dramatically reduced all three luminescence decay times, as previously reported for the A_{T1} and A_{T2} emissions.[5] The magnetic field dependence, like the temperature dependence, was the same for both A_{T1} and A_{T2} emission decay times within our experimental error, although Fukuda and Yuster[5] reported a small difference (<5%). With the field applied parallel to a $\langle 001 \rangle$ direction, both A_{T1} and A_{T2} emissions showed a compound (two-component) decay: one of the two decay-time constants being field independent and equal to the decay time measured at zero field; the other time constant depending strongly on the magnitude of the applied field and decreasing with increasing field. With the magnetic field applied along a $\langle 111 \rangle$ direction, only a single-component (field-dependent) decay was observed for both A_{T1} and A_{T2} emissions. However, in the case of the R band, both $\langle 001 \rangle$ and $\langle 111 \rangle$ field orientations gave rise to two-component decays, both components of which were field dependent as shown in Fig. 6.

V. DISCUSSION

For purposes of convenience and clarity the following discussion is divided into three sections. In the first section we shall discuss the relative magnitudes of SO and JT in the relaxed excited states A_{T1} and A_{T2} of the Sn^{2+}-vacancy complex. We then show that the presence of a nearby cation vacancy leads to two different energy-level schemes for the RES in the two extremes of SO< JT and SO> JT. Comparison with the kinetics of the luminescence decay shows that SO< JT for KI:Sn^{2+}. The second part is a discussion of the possible origins of the R emission. In the final section we give an analysis of the kinetics of the decay times and its dependence on an applied magnetic field. From this point we shall see that the R band is probably due to Sn^{2+} dimers oriented along $\langle 110 \rangle$ crystal directions.

A. Effect of SO and JT coupling on the RES of Sn^{2+}-vacancy complexes

From published polarization studies[4,9] it is clear that the JT coupling to the E_g modes is strong and that the vacancy effect may be treated as a perturbation relative to both SO and JT. We consider here the two extreme cases for which calculations can easily be carried out:

(1) vacancy effect, JT $\ll$ SO, and
(2) vacancy effect, SO $\ll$ JT.

In the following treatment we consider only linear JT coupling to E_g modes.

1. Vacancy effect, JT $\ll$ SO

Consider first an isolated Sn^{2+} ion in a site of O_h symmetry. The left-hand side of Fig. 7 shows the unrelaxed excited states of the excited configuration $(ns)(np)$ which are the triplet spin states $A_{1u}(^3P_0)$, $T_{1u}(^3P_1)$, $E_u + T_{2u}(^3P_2)$, and the singlet spin state $T_{1u}(^1P_1)$, where the free-ion terms are included in parentheses. In terms of this diagram (Fig. 7, left side) the characteristic A, B, and C absorption bands for Tl^+-like ions (see for example Fowler[1]) are

$A_{1g}(^1S_0) \rightarrow T_{1u}(^1P_1)$: C band, electric dipole allowed.

$A_{1g}(^1S_0) \rightarrow T_{1u}(^3P_1)$: A band, spin forbidden but allowed through SO coupling.

$A_{1g}(^1S_0) \rightarrow E_u + T_{2u}(^3P_2)$: B band, both electric dipole and spin forbidden but allowed by the combined effect of SO and electron-lattice coupling.

The basis functions for the triplet states A_{1u} and T_{1u} (hereafter, since we are only discussing the triplet states we shall drop the free-ion notation) are

$$
\begin{aligned}
|A_{1u}\rangle &= (Xx + Yy + Zz)/\sqrt{3}\,, \\
|T_{1u,x}\rangle &= (Yz - Zy)/\sqrt{2}\,, \\
|T_{1u,y}\rangle &= (Zx - Xz)/\sqrt{2}\,, \\
|T_{1u,z}\rangle &= (Xy - Yx)/\sqrt{2}\,,
\end{aligned}
\tag{1}
$$

where (X, Y, Z) and (x, y, z) are, respectively, sets of orbital and spin functions spanning the

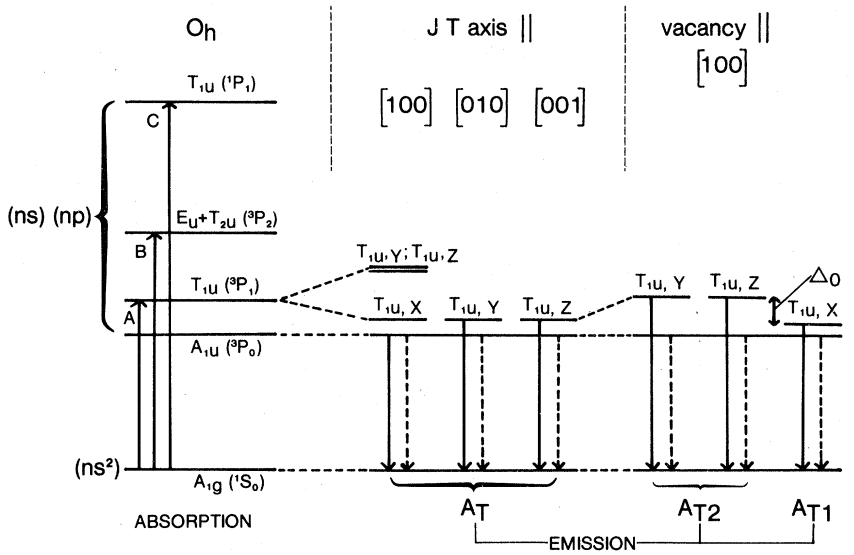

FIG. 7. The energy-level scheme for the $^3T_{1u}$ RES of KI:Sn^{2+} for JT $\ll$ SO. Left side: unrelaxed excited states; center: relaxed excited state after coupling to E_g modes; right side: effect of perturbing cation vacancy in NNN position, assuming well-localized p orbitals.

T_{1u} irreducible representation (of O_h). The states defined in Eq. (1) above are appropriate, as a first approximation, for the relaxed excited states when JT $\ll$ SO. Now consider the effect of the JT coupling (as a perturbation) on these states:

$|A_{1u}\rangle$ is unaffected.

$|T_{1u}\rangle$ states: JT coupling to the E_g modes leads to three equivalent tetragonal distortions and the system may be stabilized in any one of the T_{1u} states (see center portion of Fig. 7).

Now consider the perturbing effect on this scheme of a charge-compensating cation vacancy. Such a defect carries an effective negative charge and so, if the p orbitals of the Sn^{2+} ion are well localized, a vacancy in the NNN position (along [100]) will decrease the energy of the $T_{1u,x}$ state by an amount Δ_0 with respect to the $T_{1u,y}$ and $T_{1u,z}$ states (see right-hand side of Fig. 7). Under the same circumstances a vacancy in the NN cation site along [011] will raise the energy of the $T_{1u,x}$ state relative to the other two states. The level scheme is therefore similar to that illustrated in Fig. 7 but with the opposite sign for Δ_0. Whether the cation vacancy is in one of the six equivalent NNN sites or in one of the 12 equivalent NN sites, the result is that one of the T_{1u} states will be higher or lower in energy than the other two. This accounts for the observed double emission, A_{T1} and A_{T2}; the magnitude of the cation-vacancy perturbation, Δ_0, may be found from the splitting between A_{T1} and A_{T2} which is 0.18 eV in KI: Sn^{2+}.

Finally, we consider the kinetics of the luminescence decay from these relaxed excited states. As can be seen in Fig. 7, the nonradiative A_{1u} state lies beneath the T_{1u} states, which are radiative due to SO mixing with the singlet state. However, mixing with T_{1u} and/or $E_u + T_{2u}$ by electron-lattice coupling[15] or hyperfine interaction,[16] for example, can allow radiative decay from A_{1u}. Whatever the mixing mechanism, A_{1u} is metastable relative to T_{1u}. Since these states are interconnected by nonradiative transitions (spin-lattice relaxation processes), the kinetics of the luminescence decay following pulsed excitation into the A band will be characterized by the energy separation D between A_{1u} and T_{1u} (this will be treated in more detail below). Therefore, if SO $\gg$ JT, one should expect different behavior for the kinetics of the luminescence decay of A_{T1} and A_{T2} since the energy separation D, between the radiative (T_{1u}) levels and the metastable trap level (A_{1u}) differs by an amount $\Delta_0 = 0.18$ eV for these two emission bands (see Fig. 7). This, however, was not borne out by the results of the decay-time measurements which showed the same temperature dependence for both A_{T1} and A_{T2} within our experimental error (~5%) as shown in Fig. 5.

2. *Vacancy*, SO $\ll$ JT

Again we use a perturbation approach and, at first, neglect spin by considering the JT effect on an orbital triplet (X, Y, Z) in O_h symmetry.[17] This induces tetragonal distortions of the octahedral configuration. A [100] JT distortion lowers the energy of the X state by an amount E_{JT} and

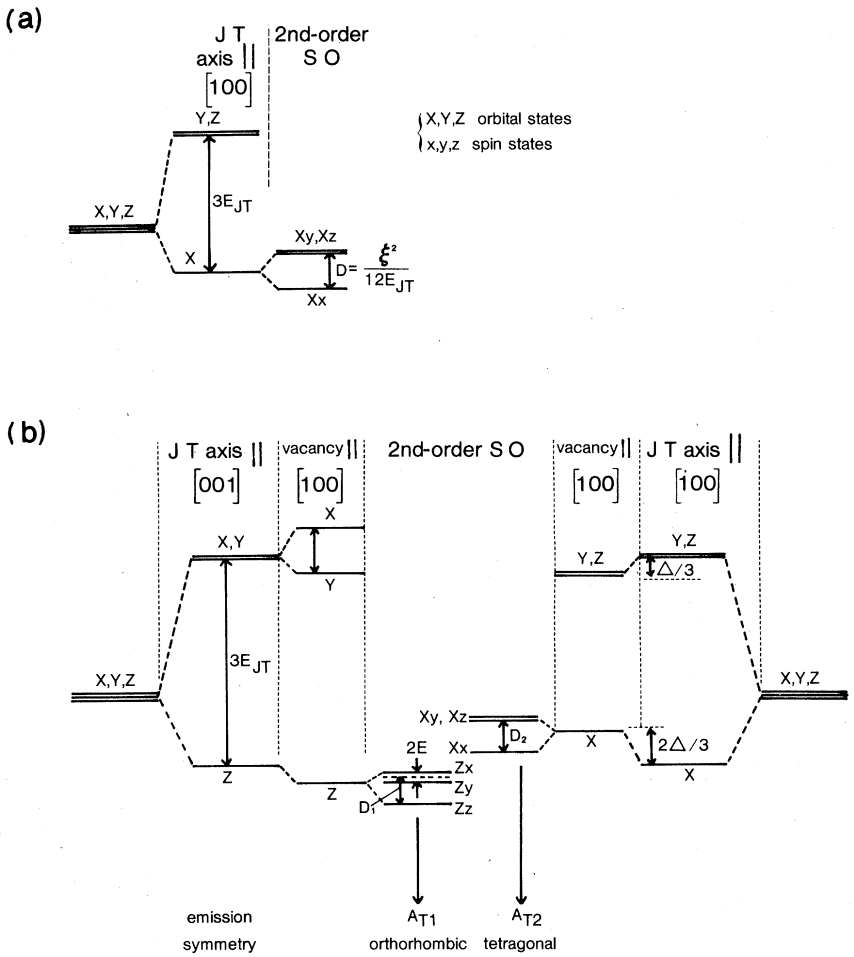

FIG. 8. (a) The energy-level scheme for the RES of an orbital triplet in O_h symmetry with JT ≫ SO. (b) The effect on (a) of a perturbing cation vacancy in the NNN position, assuming well-localized p orbitals.

raises the energy of the Y and Z states by $2E_{JT}$ [see Fig. 8(a)]. Analogous results hold true for JT distortions along [010] or [001] axes. Each of the relaxed excited states X, Y, Z has a threefold degeneracy in spin which is partially lifted by SO coupling in second order (the first-order SO perturbation being zero). In the limit of static JT effect, this results in a fine-structure separation D given by[17]

$$D = \xi^2/12E_{JT}\ , \tag{2}$$

where ξ is the SO coupling constant for a p electron. Figure 9 shows the connection between the triplet state before relaxation (absorption) and after relaxation (emission). Note that the Xx, Yy, and Zz states are the lowest states in the JT wells and since $(Xx + Yy + Zz)$ transforms as the A_{1u} representation these states are metastable.

The effect of a vacancy in the NNN position is shown in Fig. 8(b). (A similar calculation can be made for a vacancy in the NN position.) If the p orbitals of the Sn^{2+} ion are well localized, a cation vacancy along the [100] direction will raise the energy of X and decrease the energy of Y and Z, the total splitting between the X and Y states being

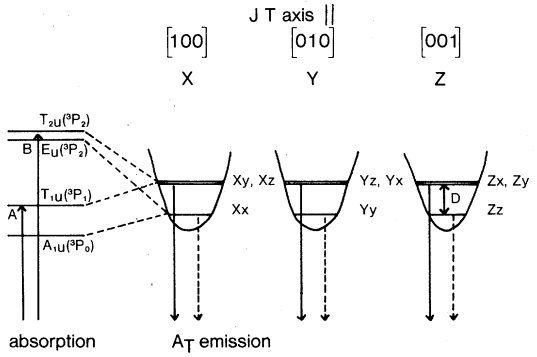

FIG. 9. Connection between the triplet state before relaxation (absorption) and after relaxation (emission) when JT ≫ SO.

Δ [Fig. 8(b)]. Two types of relaxed NNN Sn^{2+} centers are possible:

(i) *orthorhombic* centers, in which the JT distortion is perpendicular to the direction of the vacancy (as just described) and

(ii) *tetragonal* centers, in which the JT distortion is parallel to the vacancy direction.

As shown in Fig. 8(b) the orthorhombic centers are responsible for the low-energy emission (A_{T1}) while the tetragonal centers are responsible for the high-energy emission (A_{T2}), provided the vacancy is indeed the NNN position along one of the cubic axes.

The second-order spin-orbit coupling perturbation for NNN centers is also shown in Fig. 8(b). The resulting fine structure of these centers is

orthorhombic (A_{T1}):

$$D_1 = D(1-\epsilon), \quad E = \epsilon D ,$$

tetragonal (A_{T2}): (3)

$$D_2 = D(1+2\epsilon) ,$$

where $\epsilon = \Delta/6\ E_{JT}$ and D is given above by Eq. (2). Should the vacancy be in the NN position then the level schemes for A_{T1} and A_{T2} in Fig. 8(b) are interchanged. Since the emission shows only two overlapping bands we may conclude either that only one kind of center is present (NNN or NN) or that the magnitude of the cation-vacancy perturbation Δ is not very different for the two cases. Thus the splitting due to the vacancy Δ is given approximately by the separation between A_{T1} and A_{T2} emissions which is 0.18 eV in KI:Sn^{2+}. E_{JT} may be estimated from half the Stokes shift, which is 1.25 eV. Consequently $\epsilon \simeq 0.05$. This means that the difference in the fine structure of the A_{T1} and A_{T2} RES is too small to be detected in our measurements of decay times, in complete agreement with our results. We therefore conclude that the JT perturbation is much larger than the spin-orbit coupling in Sn^{2+} dissolved in KI. It should be noted that this conclusion holds true whether we have only NN, only NNN, or both complexes, since the two kinds of complexes cannot be distinguished from decay-time measurements.

B. Origin of the *R* band

The second model described in *A* agrees satisfactorily with all the available experimental information concerning the green emission doublet but does not account for the appearance of the red emission. Four possible models for the emitting state responsible for the *R* band come to mind: (i) a relaxed exciton, (ii) a second type of RES which coexists with the RES A_{T1}, A_{T2} discussed above, (iii) the RES of cubic isolated Sn^{2+} centers (with no nearby vacancy), and (iv) Sn^{2+} dimers, that is, two Sn^{2+}-cation vacancy complexes in close association. These four models are discussed successively below.

(i) Although it was the excitation of the *R* emission in the *D*-band region that first caused us to consider an exciton model this should be ruled out because the peak in the excitation spectrum of the *R* emission occurs at 330 nm which is well below the excitonic absorption band.

(ii) Tl^+-like ions quite commonly display two types of RES (usually called A_X and A_T in order of increasing energy) which are attainable by excitation into the *A* absorption band (see Fukuda[1] and also Refs. 18 and 19). The *R* emission occurs in the correct spectral region for it to be identified with an A_X type of RES. However, this cannot be the case as it is not excited by absorption into the *A* band.[11]

(iii) Optical studies of isolated Sn^{2+} centers in KBr and KCl have been made by Zazubovich.[7] He found that (a) the A_T emission related to isolated Sn^{2+} centers does occur on the low-energy side of the A_{T1} and A_{T2} emissions from Sn^{2+}-cation vacancy complexes and (b) the excitation spectrum of A_T is shifted to lower energy relative to that of A_{T1} and A_{T2}. If this were also true for KI:Sn^{2+}, emission from isolated Sn^{2+} centers should be observed by exciting below the *A* absorption band which peaks at 345 nm (see Fig. 4). Actually we found that the *R* band is not excited below *A*-band but at higher energies, and so we ruled out the isolated Sn^{2+}-center model for the *R* emission.

(iv) Finally, we consider the hypothesis that the *R* band is due to emission from Sn^{2+} dimer centers. There is evidence in favor of this model in the observation that in KBr:Sn^{2+} (which also shows a very similar *R* band) the *R* band is almost absent in freshly quenched specimens but over the course of a few days at room temperature, the A_{T1}, A_{T2} intensity decreases and that of the *R* band at first increases and then remains constant. These observations are consistent with the growth of dimers from Sn^{2+}-cation vacancy complexes and the attainment of a steady state in which the continued formation of dimers matches their aggregation to larger clusters.[21] Similarly, the *R* band is absent, or very weak, in freshly quenched KI:Sn^{2+} but forms on annealing at room temperature over a period of days.

C. Kinetics of the emission decay

We consider first the kinetics of the luminescence decay of the A_{T1} and A_{T2} bands. Since A_{T1} and A_{T2} exhibit the same kinetics, we feel justified in neglecting the vacancy effect in the following discussion, and use the model shown in Fig. 8(b).

As a result of the level structure [Fig. 8(b)] and the selection rules described above, pulsed excitation into the A absorption band should result in a two-component decay.[21-23] In many cases of ns^2 ions in alkali halides, including KI:Sn^{2+}, the short component is too short to be readily observed (<1 μsec) and the following discussion pertains only to the slow component. Considering, for example, the RES in the Z JT well, we define the rate constants for radiative transitions to the ground state A_{1g} from the trap Zz as $k_1 = 1/\tau_1$ and from the doublet (Zx, Zy) as $k_2 = 1/\tau_2 \gg k_1$. The rates for nonradiative transitions between the doublet and the trap are defined as k_{21} $(Zx, Zy \rightarrow Zz)$ and k_{12} $(Zz \rightarrow Zx, Zy)$. If relaxation between RES takes place by a direct one-phonon process, then

$$k_{12} = K\bar{n}, \quad k_{21} = K(\bar{n}+1), \tag{4}$$

where K is a constant and $\bar{n} = [\exp(D/kT) - 1]^{-1}$, and D is the energy separation between the trap and the doublet. It can be shown that the temperature dependence of the slow component of the decay, τ_s, is described by (in order of increasing temperature):

$$\frac{1}{\tau_s} = \begin{cases} k_1 & \text{when } k_{12} \ll k_1 \ll k_2 \quad (kT \ll D) \\ \dfrac{g k_{12} k_2}{k_{21} + k_2} & \text{when } k_1 \ll k_{12} \ll k_2 \\ \dfrac{g}{1+g} k_2 & \text{when } k_1 \ll k_2 \ll k_{12} \simeq k_{21} \quad (kT \gg D), \end{cases} \tag{5}$$

where $g = g_2/g_1$ is the ratio of degeneracies (i.e., $g = 2$ in the present case). In the intermediate regime $(k_1 \ll k_{12} \ll k_2)$ and at low temperatures when $kT \ll D$, Eq. (5) becomes

$$\frac{1}{\tau_s} = \frac{g k_{12} k_2}{k_{21} + k_2} \simeq \left(\frac{gKk_2}{K + k_2}\right) \exp\left(\frac{-D}{kT}\right). \tag{6}$$

From the foregoing discussion, the radiative decay time of the trap, τ_1, can be obtained from the plateau region at very low temperatures (Fig. 5). The fine structure, D, is readily determined from the experimental temperature dependence of the decay time in the region of temperature over which $\ln\tau_s$ vs $1/T$ is linear [Eq. (6)]. Finally, if measurements can be made at high enough temperatures (so that $kT \gg D$), the radiative lifetime of the doublet, τ_2, can be determined. All these parameters (D, τ_1, and τ_2) could be obtained as described above for the A_{T1}, A_{T2} emissions and these results are listed in Table I.

The kinetics of the R emission band are qualitatively the same as for the A_{T1}, A_{T2} emission (see Fig. 5), thus indicating the presence of a trap underlying a radiative level. As in the case of the A_{T1} and A_{T2} emissions the decay time of the R band (at constant low temperature ~3.3 K) changed dramatically under an applied magnetic field (see Fig. 5). Thus, despite the lack of a clear model for the R-band RES we assume it has an energy-level structure which is qualitatively similar to that of the A_{T1} and A_{T2} RES, and its decay kinetics can thus be analyzed using Eqs. (5) and (6). Unfortunately, however, the intensity of the R emission is too low at temperatures above ~20 K to permit the determination of τ_2, the decay time of the radiative doublet. An upper limit can be obtained for τ_2 from the decay time measured at 20 K (6 μsec), $\tau_2 \lesssim 4$ μsec, using Eq. (5) and assuming that $g = 2$ for the R-band RES as it does for A_{T1} and A_{T2}. The parameters for the R band resulting from the foregoing analysis are included in Table I.

TABLE I. Parameters obtained from the temperature dependence of the decay times of the A_{T1}, A_{T2}, and R emission bands in KI: Sn^{2+}.

Emission Band	D (cm^{-1})	τ_1 (μsec)	τ_2 (μsec)
A_{T1} A_{T2}	32.9	2800	0.7
R	17.9	680	$\lesssim 4$

We now turn our attention to a discussion of the magnetic field effect on the decay times. The kinetics of the luminescence decay from a system having the energy-level scheme described above may be drastically altered by the application of an external magnetic field as a result of two causes[5,13,16,24,25]:

(1) changes in the energy-level structure resulting in an alteration of the spin-lattice relaxation rate and

(2) mixing between RES resulting in an alteration of their radiative lifetimes.

Magnetic field effects of the first type can be neglected for KI:Sn^{2+} centers because the fine structure D is very large ~30 cm^{-1} (see Table I) compared to the Zeeman effect ($g\mu_B H \sim 5$ cm^{-1} assuming $H = 5.0$ T and $g = 2$). Magnetic field effects of the second type have already been described for RES of Tl^+-like ions with tetragonal and trigonal symmetry when SO$\ll$ JT (see Refs. 13 and 16). Those results can be directly applied here, since we have shown that for Sn^{2+}-vacancy complexes SO$\ll$ JT and that the vacancy effect on fine structure is negligibly small. According to Refs. 13 and 16, the radiative lifetime τ of the metastable state, e.g., Xx for the tetragonal JT well X, when perturbed by an applied magnetic field H can be described by

$$\frac{1}{\tau_s}(H)=\frac{1}{\tau_1}+a\left(\frac{g_\perp \mu_B H}{D}\right)^2\frac{1}{\tau_2}\ , \tag{7}$$

where τ_1 and τ_2 are the radiative lifetimes of the singlet Xx and doublet (Xy, Xz) at zero field, respectively, $g_\perp$ is the component of g perpendicular to the JT axis (OX) of the emitting center, and a is an angular factor depending on the relative orientations of the field H and the symmetry axis, OX. Let (α,β,γ) be the direction cosines of H in the coordinate axes OX, OY, OZ, then $a=\beta^2+\gamma^2$ for the X center. That is, only the component of the field perpendicular to the symmetry axis of the emitting center is effective in the mixing of the radiative and metastable levels of the RES. With the field applied along ⟨111⟩, and for a trigonal center, there will be a field-dependent component for only three of the four different ⟨111⟩ centers, the fourth (parallel to the field) will be unaffected. The same field orientation (⟨111⟩) will affect equally all three possible orientations of a tetragonally (⟨100⟩) distorted center. On the other hand, if the field is applied along a ⟨100⟩ direction, all four orientations of trigonal centers will be equally affected, but only two of the three tetragonal centers.

In agreement with the foregoing discussion, the A_T emission from KI:Sn^{2+} (both A_{T1} and A_{T2}), which is known to arise from a center having a tetragonal distortion, was found to give a two-component decay when the field was applied along ⟨100⟩, with one of the components being independent of the field, while a field applied along ⟨111⟩ gave rise to a single, field-dependent decay time.[13]

As shown in Fig. 6 the R emission decay exhibits two field-dependent components for both $\vec{H}\parallel\langle 111\rangle$ and $\vec{H}\parallel\langle 100\rangle$, indicating that its symmetry axis is not along either of these directions. Therefore the most likely model for the R emission is a tin dimer, oriented along a ⟨110⟩ direction, and we should consider the effect of a ⟨111⟩ and ⟨100⟩ field on a spin triplet system $S=1$ with axial symmetry along a ⟨110⟩ direction. In this case the two-component decay times would both be field dependent, with the decay times given by Eq. (7) but with the angular factor, a, having two different values (a_f and a_s) for each field orientation. The values of the angular factor (determined as in Ref. 13) for centers of ⟨111⟩, ⟨100⟩, and ⟨110⟩ symmetry in both field orientations, ⟨100⟩ and ⟨111⟩, are given in Table II. It should be noted that for the ⟨110⟩ center in a ⟨100⟩ field there will be twice as many centers having a_s as a_f, while with a ⟨111⟩ field there will be equal numbers of centers with a_s and a_f. Thus it is experimentally more difficult to determine the fast field-dependent component for a ⟨100⟩ field than for a ⟨111⟩ field. Conversely, the best conditions for measuring $\tau_s(H)$ are with the field in the ⟨100⟩ direction. Using Eq. (7), and the values of a_s and a_f from Table II, the slopes of $1/\tau_s(H)$ vs H^2, $S^{\langle ijk\rangle}$, as determined from Fig. 6, are (in $S^{-1}T^{-2}$)

TABLE II. Values of the angular factor for H along ⟨111⟩ and ⟨100⟩ and emitting centers with symmetry axis along ⟨111⟩, ⟨100⟩, and ⟨110⟩. In the last case the two angular factors which arise are labeled a_f and a_s indicating, respectively, a fast and slow field-dependent component.

	Type of center			
	⟨111⟩	⟨100⟩	⟨110⟩	
$\vec{H}$ along	a	a	a_f	a_s
⟨111⟩	$\frac{8}{9}$	$\frac{2}{3}$	1	$\frac{1}{3}$
⟨100⟩	$\frac{2}{3}$	1	1	$\frac{1}{2}$

$$\begin{aligned}
S_s^{\langle 111\rangle} &= \frac{1}{3}\frac{1}{\tau_2}g_\perp^2\left(\frac{\mu_B}{D}\right)^2=(3.9\pm 1)\times 10^2,\\
S_f^{\langle 111\rangle} &= \frac{1}{\tau_2}g_\perp^2\left(\frac{\mu_B}{D}\right)^2=(1.3\pm 0.3)\times 10^3,\\
S_s^{\langle 100\rangle} &= \frac{1}{2}\frac{1}{\tau_2}g_\perp^2\left(\frac{\mu_B}{D}\right)^2=(5.8\pm 0.1)\times 10^2,\\
S_f^{\langle 100\rangle} &= \frac{1}{\tau_2}g_\perp^2\left(\frac{\mu_B}{D}\right)^2=(1.4\pm 0.4)\times 10^3.
\end{aligned} \tag{8}$$

The errors indicated in those slopes are indicative of the difficulties described above. However, it is comforting that the values of slopes given in Eqs. (8) all lead to the same value of $g_\perp/\tau_2$ (within respective experimental errors). Thus, within the experimental uncertainties, it seems that the R emission arises from a spin triplet within a ⟨110⟩ oriented RES. Using $S_s^{\langle 100\rangle}$ (which is the most accurately measured slope) and the value of τ_2 given in Table I, we obtain the limiting value of $g_\perp$ for the RES of the R emission as $g_\perp \leq 2.6$.

VI. CONCLUSIONS

From the results described above and the preceding discussion we are led to conclude that the A_{T1} and A_{T2} emissions from KI:Sn^{2+} must arise from an RES in which electron-lattice coupling (or JT effect) is greater than the spin-orbit interaction. This RES is then, in turn, further perturbed by the electrostatic effect of a nearby cation vacancy. The location of the cation vacancy (NN and/or NNN) is still an open question.[4,10,14] Our model is based on the JT perturbation being much larger than the SO coupling and includes an axial perturbation due to a nearby cation vacancy. The decay-time measurements confirm the result-

ing level scheme but we cannot decide, from the data presented here, whether the vacancy is in the NN or the NNN position (or both) with respect to the Sn^{2+}. We hope that current polarization measurements will help to elucidate the problem. The new red emission, R, is most likely due to spin triplet states of Sn^{2+} dimers oriented along ⟨110⟩.

ACKNOWLEDGMENTS

We would like to acknowledge the value of conversations with Professor W. B. Fowler. We are also most grateful to Dr. P. H. Yuster and Professor A. Fukuda for gifts of single crystals of KI:Sn^{2+} and to Dr. P. W. Levy for neutron-activation analysis. We thank the Natural Sciences and Engineering Research Council for financial support, both in the form of individual operating grants and as a cooperative grant. The authors also wish to acknowledge the Quebec Ministry of Intergovernmental Affairs and the Ministry of Education of Ontario for support under the auspices of the Quebec-Ontario exchange program. Y.K. is grateful to Kobe University for leave of absence.

*Permanent address: Department of Physics, Kobe University, Rokkodai-cho, Nada-ku, Kobe 657, Japan.

[1]For a review see W. B. Fowler, in *Physics of Color Centers*, edited by W. B. Fowler (Academic, New York, 1968), p. 54; A. Fukuda, Phys. Rev. B 1, 4161 (1970).
[2]A. Fukuda, K. Inohara, and R. Onaka, J. Phys. Soc. Jpn. 19, 1274 (1964).
[3]K. O. Gannon and P. W. M. Jacobs, J. Phys. Chem. Solids 36, 1375 (1975); 36, 1383 (1975).
[4]A. Fukuda, Phys. Rev. Lett. 26, 314 (1971).
[5]A. Fukuda and P. Yuster, Phys. Rev. Lett. 28, 1032 (1972).
[6]A. Fukuda, Solid State Commun. 12, 1039 (1973).
[7]S. G. Zazubovich, Opt. Spektrosk. 37, 711 (1974) [Opt. Spectrosc. (USSR) 37, 404 (1974)].
[8]V. Hizhnyakov, S. Zazubovich, and T. Soovik, Phys. Status Solidi B 66, 727 (1974).
[9]V. Hizhnyakov and S. Zazubovich, Phys. Status Solidi B 86, 733 (1978).
[10]E. Realo and S. Zazubovich, Phys. Status Solidi B 57, 69 (1973).
[11]P. W. M. Jacobs, Y. Kamishina, L. L. Coatsworth, and M. J. Stillman, J. Lumin. 18/19, 619 (1979).
[12]D. J. Simkin, K. O. Gannon, J. P. Martin, Y. Kamishina, and P. W. M. Jacobs, J. Lumin. 18/19, 623 (1979).
[13]D. J. Simkin, J. P. Martin, Le Si Dang, and Y. Kamishina, Chem. Phys. Lett. 65, 569 (1979).
[14]C. J. Delbecq, R. Hartford, D. Schoemaker, and P. H. Yuster, Phys. Rev. B 13, 3631 (1976).
[15]W. B. Fowler, Phys. Status Solidi 33, 763 (1969).
[16]Y. Merle d'Aubigné and Le Si Dang, Phys. Rev. Lett. 43, 1023 (1979).
[17]F. S. Ham, Phys. Rev. 138, A1727 (1965).
[18]M. Bacci, A. Ranfagni, M. Cetica, and G. Viliani, Phys. Rev. B 12, 5907 (1975).
[19]Le Si Dang, R. Romestain, Y. Merle d'Aubigné, and A. Fukuda, Phys. Rev. Lett. 38, 1539 (1977).
[20]A. Scacco and P. W. M. Jacobs (unpublished).
[21]R. Illingworth, Phys. Rev. 136, A508 (1964).
[22]M. F. Trinkler and I. K. Plyavin, Phys. Status Solidi 11, 277 (1965).
[23]D. Le Si Dang, R. Romestain, D. Simkin, and A. Fukuda, Phys. Rev. B 18, 2989 (1978).
[24]W. B. Fowler, M. J. Marrone, and M. N. Kabler, Phys. Rev. B 8, 5909 (1973).
[25]H. Takazoe, S. Hirako, and R. Onaka, J. Lumin. 16, 213 (1978).